Optical Engineering 46(8), 1 (August 2007)

Binary-phase micrograting and polarization beamsplitter for free-space micro-optical pickups

Chi-Hung Lee
National Chiao Tung University
Department of Photonics and Institute of
Electro-optical Engineering
Hsin-Chu 300, Taiwan, R.O.C.
E-mail: tainanncku@hotmail.com

Yi Chiu
National Chiao Tung University
Department of Electrical and Control
Engineering
Hsin-Chu 300, Taiwan, R.O.C.
E-mail: yichiu@mail.nctu.edu.tw

Han-Ping D. Shieh
National Chiao Tung University
Department of Photonics and Display
Institute
Hsin-Chu 300, Taiwan, R.O.C.

Abstract. A pop-up binary-phase micrograting and a pop-up micro polarization beamsplitter, for potential use in micro-optical pickups, have been realized on a single silicon chip using a two-layer polysilicon and one-layer silicon nitride micromachining process. In the case of the micrograting, a diffraction efficiency ratio between 4 and 10 can be achieved provided that the duty cycle is between 0.4 and 0.6 and the depth between 455 and 485 nm, respectively. For a grating designed for a diffraction ratio of 7, the measured ratio is 8.31. The polarization beamsplitter is a silicon nitride thin film placed at the Brewster angle. The transmittance of the TM mode was measured to be more than 98.5%, while the reflectance of the TE mode was 21.4%. [DOI: 10.1117/1.2769362]

Subject terms: binary-phase grating; polarization beamsplitter; diffraction efficiency ratio; silicon nitride; optical pickup.

Paper 060621R received Aug. 8, 2006; revised manuscript received Feb. 4, 2007; accepted for publication Feb. 20, 2007.

1 Introduction

Microgratings and micro polarization beam splitters (PBSs) are required in many micro-optical systems for sensing, data storage, and signal processing where diffraction and polarization states of light are of concern. In an optical data storage system, a micrograting can be used to divide the incident light into 0th-order and ±1st-order beams. The 0th-order beam is used for reading and writing data, while the ±1st-order beams are used for tracking servo control in the three-beam tracking method. A PBS can be used to split the light into two orthogonally polarized components, the transverse electric (TE) and transverse magnetic (TM) modes. The TM mode is for reading and writing the data on the disk; the TE mode is used for monitoring the light intensity.

Two silicon-based micromachining technologies have drawn much attention for their high degree of accuracy and monolithic integration with other optical components in micro-optical pickups. One is based on surface-micromachined microhinge technology; an out-of-plane, three-dimensional micro-Fresnel lens,[1] a micrograting, a micro-optical pickup,[2] a microetalon,[3] and other elements have been demonstrated. These elements used thin polysilicon films as the optical patterns, which are not transparent in the visible spectrum. The other technology is based on bulk micromachining, which has been used to fabricate a silicon nitride transmissive micrograting[4] and a micro-optical pickup system.[5] These devices required a silicon nitride layer as the mechanical substrate, which suffered from reflection loss.

The objective of this paper is to fabricate a binary phase micrograting and a micro-PBS, both of which are framed by pop-up polysilicon structures for micro-optical pickup operation in the visible spectrum. Low-stress silicon nitride is used for its high transparency in the visible spectrum and its superior chemical and mechanical properties.

2 Optical Design and Simulation

2.1 *Binary-Phase Micrograting*

To apply the micrograting in a micro-optical pickup, the diffraction efficiency ratio η of the 0th-order beam intensity I_0 and the ±1st-order beam intensities $I_{\pm 1}$ should be controlled to the range from 4 to 10, depending on the requirement of the servo control system. In addition, the energy utilization efficiency, $\eta_u = (I_{-1} + I_0 + I_{+1}) / \Sigma_l I_l$, where $\Sigma_l I_l$ is the total intensity of the diffracted beams, should be as high

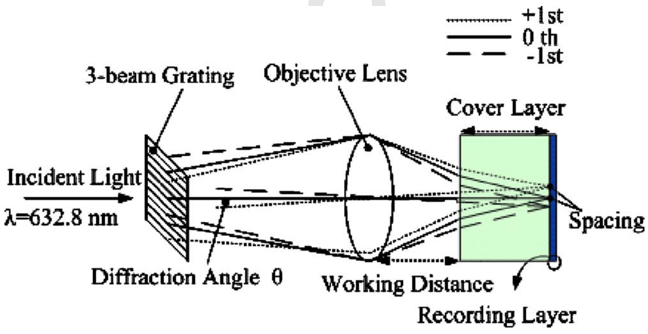

Fig. 1 Schematic of the three beams from a micrograting used for reading and tracking a disk. The working distance, the thickness of the cover layer, and the spacing between the diffraction beams on the disk determine the first-order diffraction angle θ, which is related to the depth and the period of the micrograting and to the wavelength of the incident light.

0091-3286/2007/$25.00 © 2007 SPIE

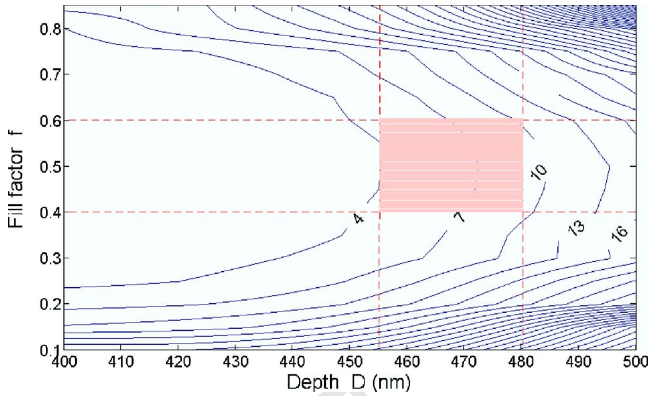

Fig. 2 Diffraction ratio ($I_0/I_{\pm1}$) contours for various values of the fill factor f and of the grating depth D. The shaded rectangle represents diffraction ratios between 4 and 10. If the grating period is 8 μm and linewidth is 4 μm, the process margins of f and D are as high as 0.5±0.1 and 467.5±12.5 nm, respectively.

as possible.[6] The diffraction angle is determined by the optical system layout parameters, such as the working distance, the thickness of the cover layer of the disk, and the spacing between the 0th-order beam and the ±1st-order beams on the disk, as shown in Fig. 1.

To determine the diffraction angle of the first-order beams, the current design assumed 40-μm spacing on the disk. For a 200-μm-thick cover layer with refractive index 1.6, the equivalent air thickness of the cover layer is 125 μm. If the working distance between the objective lens and the cover layer is 400 μm, then under the thin-lens approximation for the objective lens, the diffraction angle θ is about 4.35 deg. For a transmissive grating with $\theta=4.35$ deg, $m=1$, and $\lambda=632.8$ nm, the period Λ is about 8.35 μm, derived from the equation $\Lambda \times \sin \theta = m \times \lambda$. Here $\Lambda = 8$ μm was selected in the design. To meet the specification, namely $\eta=4$ to 10 and high η_u for $\Lambda=8$ μm, a grating with rectangular shape was designed using the commercial software G-Solver.

The diffraction energy distribution of a grating can be determined from the period, the linewidth, and the depth of the grating, denoted by Λ, w, and D, respectively. The fill factor, $f=w/\Lambda$, is defined as the ratio of the linewidth to the grating period. Plane waves are incident normal to the grating, which is supported by a polysilicon frame. Low-stress silicon nitride is used as the grating material, with refractive index $n=2.102+0.008i$ at $\lambda=632.8$ nm.

It is found that when the fill factor is 0.50, multiple grating depths may be selected. For example, 108 nm ($\eta_u=81.7\%$), 473 nm ($\eta_u=83\%$), and 665 nm ($\eta_u=74.7\%$) satisfy $\eta=7:1$, which is the middle value of the specification. Other grating depths meeting the requirement are higher than 1000 nm, which is not suitable in surface micromachining processes. To have sufficient mechanical strength and reasonable fabrication yield, the depth 473 nm was selected, which also yields high energy utilization efficiency. The contour plot of the diffraction ratio $I_0/I_{\pm1}$ is shown in Fig. 2 for several values of D and f. A diffraction ratio between 4 and 10 is obtained provided that $0.4<f<0.6$ and 455 nm$<D<$480 nm. If the grating period is 8 μm and the linewidth is 4 μm, the process margins of f and D are as high as 0.5±0.1 and 467.5±12.5 nm, respectively.

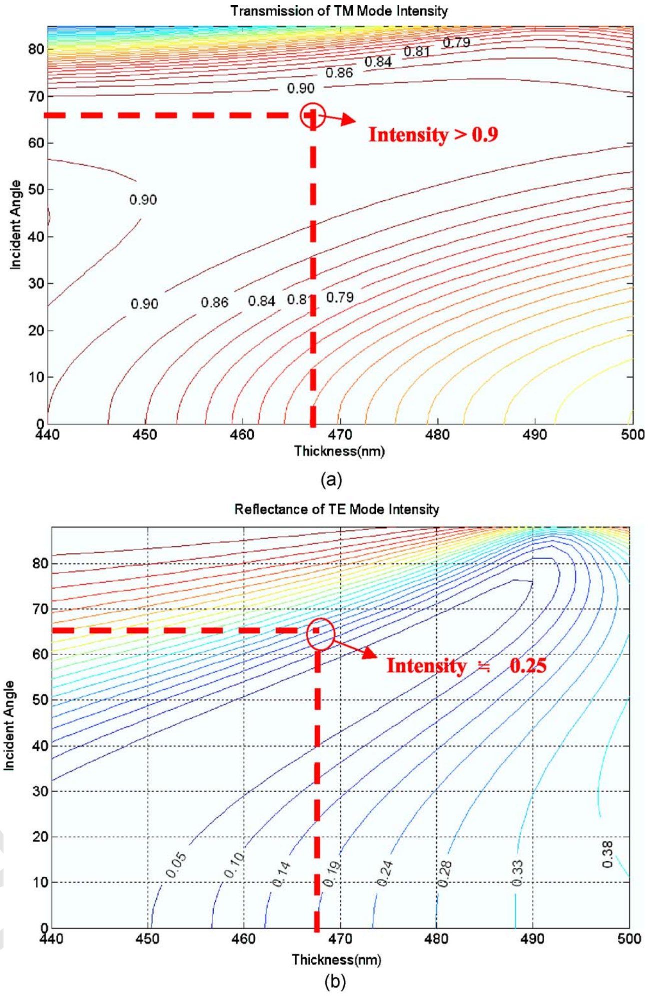

(a)

(b)

Fig. 3 Contours of (a) transmittance of the TM mode and (b) reflectance of the TE mode versus incident angle and thickness of silicon nitride. The intersection point of the dashed lines corresponds to the light incident on the micro-PBS with a thickness 467.5 nm at the Brewster angle $\theta_B=66$ deg. Under this condition, the transmission of the TM mode intensity is larger than 90%, while the reflectance of the TE mode is about 25%.

2.2 *Thin-Film PBS*

In a micro-optical pickup, the design target of the micro-PBS is to have maximum transmittance of the TM mode and detectable reflectance of the TE mode. The operation principle of the thin-film PBS is based on the polarization-dependent characteristics of the dielectric film,[7] which can be described by the characteristic matrix

$$M = \begin{bmatrix} B \\ C \end{bmatrix} = \begin{bmatrix} \cos \delta_i & -\frac{i}{\eta_i} \sin \delta_i \\ -i\eta_i \sin \delta_i & \cos \delta_i \end{bmatrix} \begin{bmatrix} 1 \\ \eta_a \end{bmatrix}, \qquad (1)$$

where

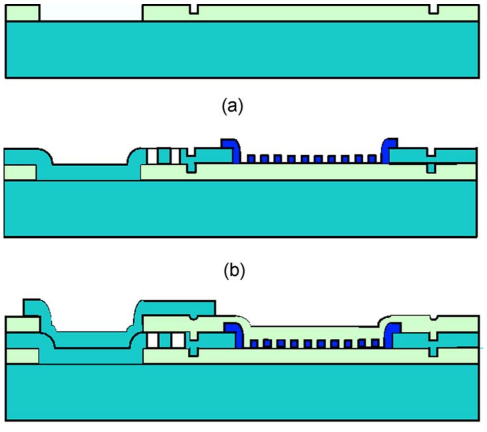
(a)
(b)
(c)

Fig. 4 Fabrication process flow of the micrograting and the micro-PBS. (a) The first dimple etch and anchor etch after the first silicon dioxide deposition. (b) Low-stress silicon nitride patterning after the first polysilicon deposition and patterning. (c) The second polysilicon deposition and patterning after the second silicon dioxide deposition and the second anchor etch.

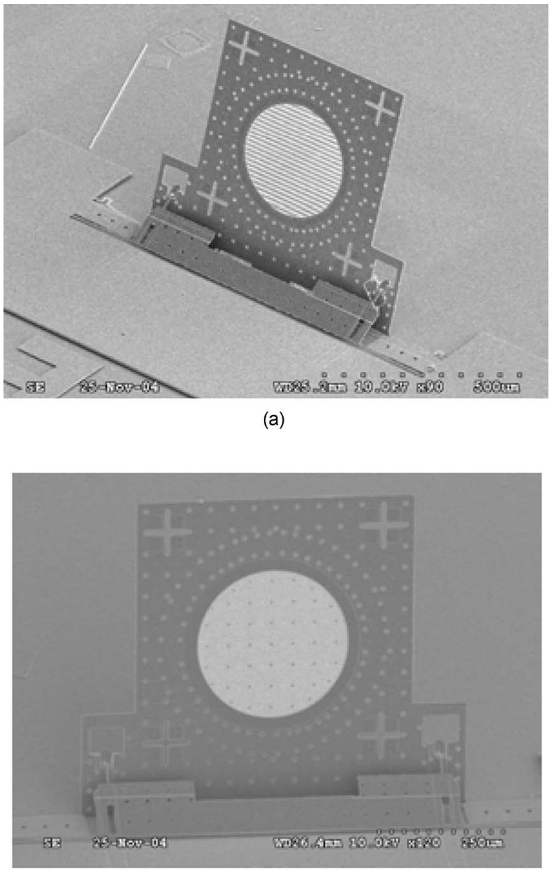

(a)
(b)

Fig. 5 SEM of a pop-up (a) micrograting and (b) micro-PBS. The sizes of the micrograting and micro-PBS are 500×600 μm^2 each. A pair of microspring latches is used to fix the microdevices nearly vertically. The optical pattern is circular with a diameter of 300 μm.

$$\delta_i = \frac{2\pi}{\lambda} N_i d_i \cos\theta_i . \tag{2}$$

Here δ_i is related to the complex refractive index N_i, the thickness d_i of the layer, the wavelength λ, and the refractive angle θ_i. The optical admittances η_i of the layer and η_a of the air substrate are given by

$$\eta_i = N_i \cos\theta_i \quad \text{for TE mode,} \tag{3}$$

$$\eta_a = \cos\theta_a \quad \text{for TE mode,} \tag{4}$$

$$\eta_i = N_i / \cos\theta_i \quad \text{for TM mode,} \tag{5}$$

$$\eta_a = 1/\cos\theta_a \quad \text{for TM mode.} \tag{6}$$

The reflectance R and transmittance T of the incident light for both polarizations can be derived from Eqs. (1) to (6):

$$R = \left(\frac{\eta_a B - C}{\eta_a B + C} \right)^2 , \tag{7}$$

$$T = \frac{4\eta_a R_e(\eta_a)}{(\eta_a B + C)(\eta_a B + C)^*} . \tag{8}$$

The transmittance of the TM mode and the reflectance of the TE mode, therefore, are functions of the thickness of the silicon nitride film and incident angle, as shown in Fig. 3(a) and 3(b). At the Brewster incidence angle, $\theta_B = \tan^{-1} n_f$, the TM polarization will totally transmit, leaving the reflected light to be pure TE polarization. For a refractive index $n_f = 2.1$ at $\lambda = 632.8$ nm, θ_B is about 66 deg. For a film thickness of 440 to 500 nm, the transmission of TM mode intensity is larger than 90% within $\theta_B \pm 10$ deg, while the reflectance of the TE mode varies significantly. In order to fabricate the micrograting and the micro-PBS on a single chip, the target thickness of the micro-PBS was 467.5 nm, the same as the grating. Under this condition, the reflectance of the TE mode is about 25%, which is small but acceptable in a practical system. The transmitted beam includes TE and TM modes. This large amount of transmitted TE mode will constitute noise; the minor-polarization crosstalk should be sufficiently low in some nonpolarized memory systems such as CD, DVD, and Blu-ray; however, it would be a problem in a polarized (e.g., a magneto-optical) memory system.

3 Fabrication

The micrograting and micro-PBS consist of low-stress silicon nitride mounted on a perpendicular polysilicon supporting frame. The measured tensile stress of the silicon nitride layer is about 50 MPa, which is low enough for optical applications.

The pop-up micrograting and micro-PBS were fabricated using the two-layer polysilicon and one-layer silicon nitride surface micromachining process shown in Fig. 4. To fabricate the devices, dimples and anchors were patterned in the sacrificial oxide layer [Fig. 4(a)]. After a microplate was formed in the structural polysilicon layer, the low-stress silicon nitride layer was patterned [Fig. 4(b)]. The second sacrificial oxide layer and structural polysilicon layer were deposited and patterned to implement the mi-

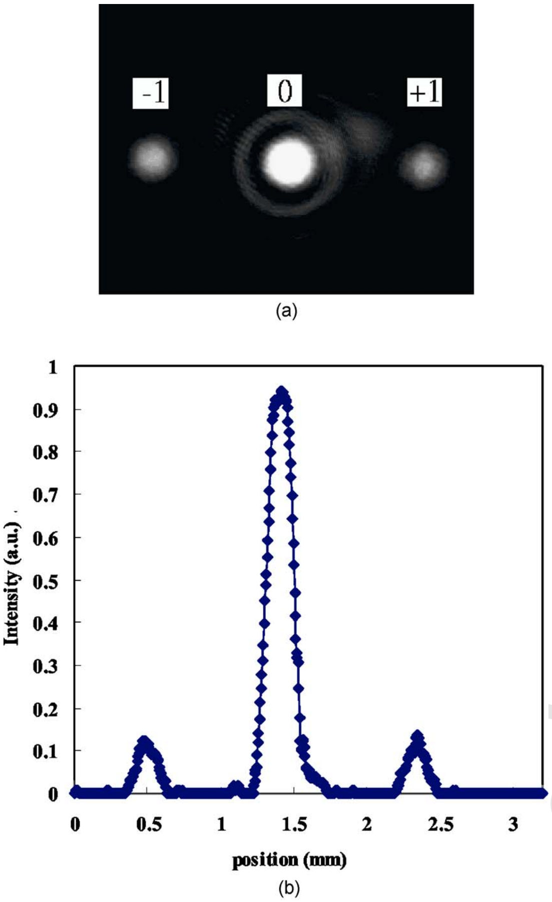

(a)

(b)

Fig. 6 (a) Diffraction pattern and (b) the cross section of its 0th-order beam and ±1st-order beams from the micrograting, measured by a CCD camera positioned 10 mm away.

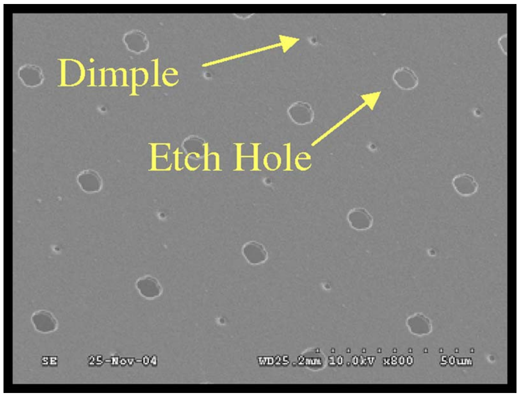

Fig. 7 SEM of etch holes and dimples in the micro-PBS. The actual shape of the two structures tends to be circular due to imperfect lithography and etching. The diameter of the etch hole is about 5 μm.

crospring latches overlapping the microplate [Fig. 4(c)]. After annealing and releasing, the micrograting and PBS were lifted to a vertical position by microprobes. Figure 5 shows the SEM photograph of the pop-up grating and the pop-up PBS. The sizes of the micrograting and micro-PBS are 500×600 μm^2 each. A pair of microspring latches is used to fix the microdevices nearly vertically (at 92 deg). The aperture is circular with a diameter of 300 μm.

4 Experimental Results and Discussion

To measure the optical performance of the micro devices, a He-Ne laser at $\lambda = 632.8$ nm was used as the light source. A polarizer was adjusted to obtain the required polarization states. The optical patterns were measured by a CCD camera positioned at 10 mm from each microdevice. For the micrograting, the measured Gaussian beam widths of the −1st-, 0th-, and +1st-order beams were 265, 290, and 270 μm, respectively, indicating symmetrical intensity distribution [Fig. 6(a)]. The measured diffraction angle at far field was 4.5 deg, which agrees well with the theoretical value of 4.53 deg. The measured diffraction efficiency ratio was 8.31 [Fig. 6(b)]. The deviation from the target value of 7.0 was mainly due to the thickness variation and to the roughness of the sidewall and the surface of the grating. The mean roughness was 4.9 nm on average, which introduced phase variation and affected the energy distribution of the diffracted beams. Under these conditions, the achieved η of 8.31 is well within the specification (4 to 10). The micrograting is thus applicable for a micro-optical pickup using the three-beam tracking method.

For the micro-PBS, the measured values of the transmittance of the TM mode and the reflectance of the TE mode at the Brewster angle were 98.5% and 21.4%, respectively. The deviation from the calculated values can be attributed to two factors: the existence of etch holes and dimples, and the thickness variation and roughness of the silicon nitride film. A close view of the micro-PBS with etch holes and dimples is shown in Fig. 7. The etch holes, which were used to release the microdevice from the substrate, reduce the reflection area by 1.5%. The dimples were used to avoid stiction between the microdevice and the substrate. Both structures also created higher-order diffraction beams and thus reduced the peak intensity of the main beams in the reflected light and the transmitted light, as shown in Fig. 8. The noises due to etch holes and dimples can be partly alleviated by randomly distributing the etch holes and dimples.[8] A detailed description of the diffraction properties of surface-micromachined devices with etch holes can be found in Ref. 9. The thickness variation and roughness of the silicon nitride film as influenced by film growth and HF releasing can cause phase differences and scattering of the light at the interface. Besides, the thermal stress between the silicon nitride film and the polysilicon plate distorted the intensity profile of the main beam.

With spring latches, the pop-up angles of the microdevices had a certain amount of deviation from 90 deg, which in turn affected the light incident angle and consequently the diffraction efficiency ratio and angular distribution. To realize a micro-optical pickup, a more precise mechanism is required to assemble the microdevices on the substrate.

5 Conclusion

Using a two-layer polysilicon and one-layer low-stress silicon nitride surface micromachining process, a binary phase pop-up micrograting and a micro-PBS were demonstrated. The size of the device is 500×600 μm with an optical pattern area 300 μm in diameter. For the micrograting, the

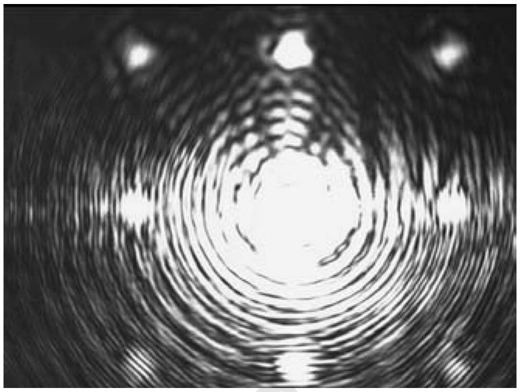

Fig. 8 CCD graph of the transmitted diffraction pattern from the micro-PBS. Higher-order diffraction beams are due to the existence of the periodic array of etch holes and dimples in the micro-PBS.

measured diffraction angle of 4.5 deg and diffraction efficiency ratio of 8.31 agree reasonably with the designed value. For the micro-PBS, the transmittance of the TM mode and the reflectance of the TE mode reached 98.5% and 21.4%, respectively. The optical performance of the microdevices shows their potential for integration with other micro-optical elements for optical storage applications.

Acknowledgments

The authors thank Prof. L. S. Huang at National Taiwan University for fruitful discussions. This work is supported by the Ministry of Economic Affairs under grant No. 93-EC-17-A-07-S1-0011.

References

1. L. Y. Lin, S. S. Lee, K. S. J. Pister, and M. C. Wu, “Three-dimensional micro-Fresnel optical elements fabricated by micromachining technique,” *Electron. Lett.* **30**(5), 448–449 (1994).
2. S. S. Lee, L. Y. Lin, and M. C. Wu, “Surface-micromachined free-space micro-optical systems containing three-dimensional microgratings,” *Appl. Phys. Lett.* **67**(15), 2135–2137 (1995).
3. L. Y. Lin, J. L. Shen, S. S. Lee, and M. C. Wu, “Micromachined three-dimensional tunable Fabry-Perot etalons,” *Proc. SPIE* **2641**, 20–27 (1995).
4. C. C. Lee, Y. C. Chang, C. M. Wang, J. Y. Chang, and G. C. Chi, “Silicon-based transmissive diffractive optical element,” *Opt. Lett.* **28**(14), 1260–1262 (2003).
5. J. Y. Chang, C. M. Wang, C. C. Lee, H. F. Shih, and M. L. Wu, “Realization of free-space optical pickup head with stacked Si-based phase elements,” *IEEE Photonics Technol. Lett.* **17**(1), 214–216 (2005).
6. H. Zhang, R. Cui, M. Gong, D. Zhao, P. Yan, and W. Jia, “Error analysis of gratings in optical pickup heads,” *Opt. Eng.* **41**(8), 1780–1786 (2002).
7. M. Born and E. Wolf, “Basic properties of the electromagnetic field,” Chap. 1 in *Principles of Optics*, Chap. 1, pp. 54–60, Cambridge Univ. Press, London (2002).
8. C. H. Tien and C. H. Lee, “Optical properties of surface micromachining with randomly distributed etch holes,” *Jpn. J. Appl. Phys.* **45**(2A), 1015–1017 (2006).
9. J. Zou, M. Balberg, C. Byrne, C. Liu, and D. J. Brady, “Optical properties of surface micromachined mirrors with etch holes,” *J. Microelectromech. Syst.* **8**(4), 506–513 (1999).

Chi-Hung Lee graduated from the Department of Materials Science and Engineering, National Cheng Kung University, in 1995, and received his master’s degree there in 1997. Since 2002, he has been with the Flat Panel Display System Laboratory, Department of Photonics & Institute of Electro-optical Engineering, National Chiao Tung University. His research interests include optical storage, diffractive optical elements, and microfabrication.

Yi Chiu is a professor in the Department of Electrical and Control Engineering, National Chiao Tung University. He received his BS in electrical engineering from National Taiwan University in 1988, his MS in electrical and computer engineering from Carnegie Mellon University in 1991, and his PhD in electrical and computer engineering from Carnegie Mellon University in 1996. He was a manager at Acer Media Technology Inc. His research interests include optical storage, integrated near-field optical heads for hybrid recording, MEMS-based electrostatic vibration-to-electric energy converters, and photonic systems on chip.

Han-Ping D. Shieh received his BS degree from National Taiwan University in 1975, and his PhD in electrical and computer engineering from Carnegie Mellon University, Pittsburgh, PA, USA, in 1987. He joined National Chiao Tung University (NCTU) in Hsinchu, Taiwan, as a professor at the Institute of Opto-Electronic Engineering and the Microelectronics and Information Research Center (MIRC) in 1992 after having been a research staff member at IBM T.J. Watson Research Center, Yorktown Heights, NY, USA, since 1988. He now is the AU Optronics Chair professor and associate director at MIRC, NCTU. He founded the Display Institute at NCTU in 2003, the first such graduate academic institute in the world dedicated to display education and research. He also has held a joint appointment as a research fellow at the Center for Applied Sciences and Engineering, Academia Sinica, since 1999. His current research interests are in display, optical MEMS, nano-optical components, and optical data storage technologies.